Jozef Kováčik, Lenka Husáková, Mihaela Vlassa, Martina Piroutková, Marek Vydra, Jan Patočka, Miuţa Filip (2023). Elemental profile identifies metallurgical pollution in epiphytic lichen Xanthoria parietina and (hypo)xanthine correlates with metals. *Science of The Total Environment*. Volume 883, 2023, 163527. DOI: 10.1016/j.scitotenv.2023.163527

Graphical Abstract

Xanthoria parietina

15 localities in Slovakia

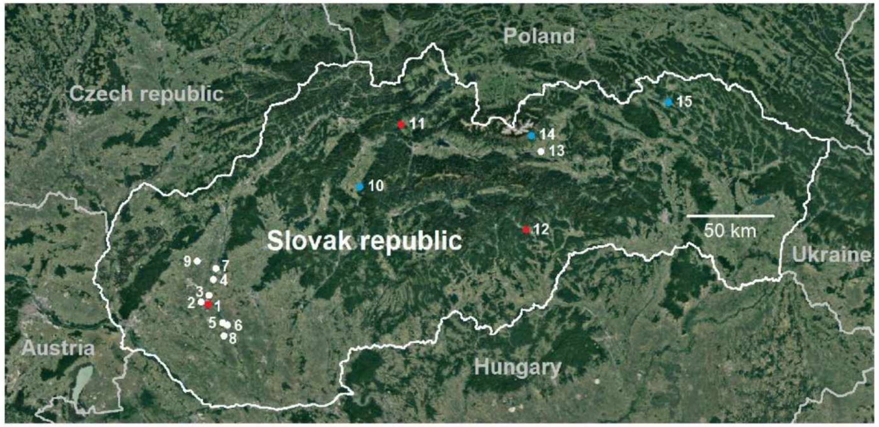

PCA with K-means enabled the grouping of samples into 4 clusters based on the content of 55 elements

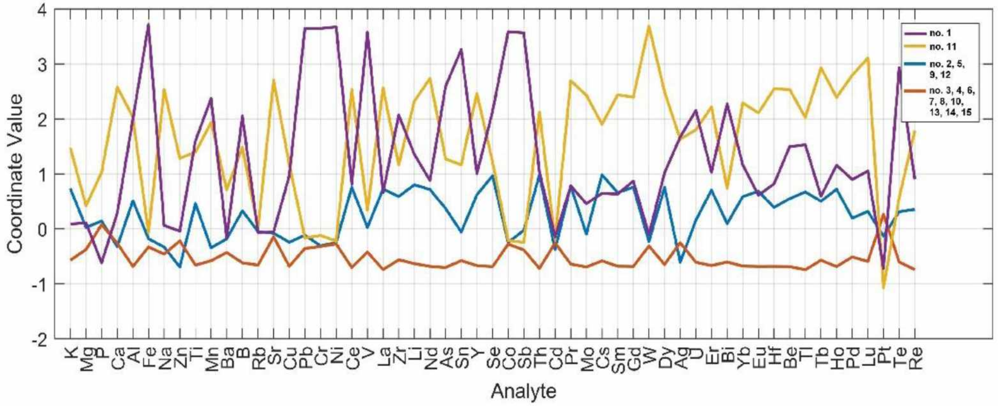

many elements had negative correlation with AsA, NPT, SP or allantoin but possitive with hypo/xanthine

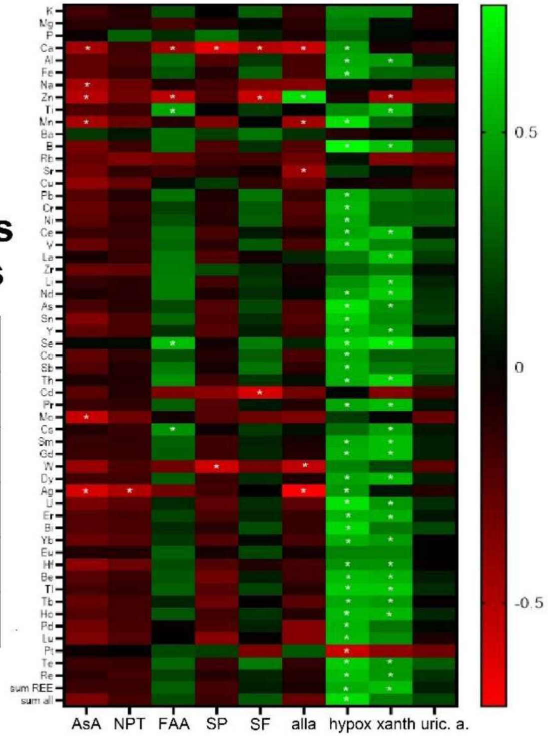

Highlights

- ► 55 elements quantified at 15 localities clearly separated metallurgical sites by PCA
- ► metallurgical sites had unique contaminants but Cd, Ba, Pt and Re need attention
- ► anthropogenic contamination (EF>10) found for P-Zn-B-As-Sb-Cd-Ag-Bi-Pd-Pt-Te-Re
- ► ascorbic acid, thiols and allantoin had rather negative correlation with elements
- ► hypo/xanthine may be protective metabolites (positive correlation with elements)

Elemental profile identifies metallurgical pollution in epiphytic lichen *Xanthoria parietina* and (hypo)xanthine correlates with metals

Jozef Kováčik [a]*, Lenka Husáková [b], Mihaela Vlassa [c], Martina Piroutková [b], Marek Vydra [a], Jan Patočka [b], Miuța Filip [c]

[a] Department of Biology, University of Trnava, Priemyselná 4, 918 43 Trnava, Slovak Republic

[b] Department of Analytical Chemistry, Faculty of Chemical Technology, University of Pardubice, Studentská 573 HB/D, 532 10 Pardubice, Czech Republic

[c] Raluca Ripan Institute for Research in Chemistry, Babeş-Bolyai University, 30 Fântânele Str., 400294, Cluj-Napoca, Romania

*corresponding author e-mail: jozkovacik@yahoo.com

https://orcid.org/0000-0002-5701-0598

Abstract

The accumulation of 55 elements in lichens under the heap of a former nickel smelter (village Dolná Streda, Slovakia) and at eight sites at different distances from the heap plus six sites throughout Slovakia was studied to determine the elemental profile. The major metals in the heap sludge and in the lichens below the heap (Ni, Cr, Fe, Mn, and Co) were surprisingly low in lichens from both the near and far vicinity of the heap (4 – 25 km), indicating limited airborne spread. However, two different sites with metallurgical activity (the other site near the ferroalloy producer in Orava) typically contained the most individual elements, including rare earth elements Th, U, Ag, Pd, Bi and Be, and their separation from another site was confirmed by PCA and HCA. In addition, the amounts of Cd, Ba and Re were highest at sites without a clear source of pollution and further monitoring is needed. It was also an unexpected finding that the enrichment factor calculated using UCC values was increased (often considerably >10) for 12 elements at all 15 sites, indicating eventual anthropogenic contamination with P, Zn, B, As, Sb, Cd, Ag, Bi, Pd, Pt, Te and Re (and other EF values were locally increased). Metabolic analyses showed a negative correlation between some metals and metabolites (ascorbic acid, thiols, phenols and allantoin), but slightly positive (amino acids) or highly positive correlation with purine derivatives hypoxanthine and xanthine. The data suggest that lichens adapt their metabolism to excessive metal loading and that epiphytic lichens are suitable for identifying metal contamination even at apparently clean sites.

Keywords: air pollution; antioxidants; lichens; PM10 particles; toxic metals; purine.

1. Introduction

Lichens are symbiotic entities typically formed by a partner symbiosis of fungi and algae, which gives the organism the ability to colonize new and often hostile environments. An epiphytic environment can also be considered such a hostile environment, however, there are many species of lichens inhabiting trees (Nannoni et al. 2015; Zakrzewska and Klimek 2018; McDonough et al. 2022; Popovici et al. 2022). The most widely studied in many countries is the genus *Xanthoria* and species *X. parietina* (Rola and Osyczka 2019; Paoli et al. 2014b; Dörter et al. 2020; Parviainen et al. 2020).

Biomonitoring of contamination using plants is used as an economically affordable alternative to various technically and financially demanding devices. Mainly leaves and needles are often used for these purposes, but lichens typically accumulate larger amounts of metals due to their slow growth and long life (Koz et al. 2010; Zakrzewska and Klimek 2018; Vannini et al. 2021). Epiphytic lichen species are also readily available indicators of pollution that are not affected by direct contamination from the soil (Kularatne and de Freitas 2013; Manninen et al. 2023). It has been observed using *Xanthoria parietina* that polluted localities may be distinguished from less polluted (Demiray et al. 2012; Dörter et al. 2020; Parviainen et al. 2020). In Slovakia, only few studies were performed e. g. in the capital city Bratislava using *Hypogymnia physodes* (Guttová et al. 2011), in 2nd largest city Košice using various lichens (Bačkor et al. 2003; Dzubaj et al. 2008) or using *Xanthoria parietina* near a cement mill (Paoli et al. 2014b).

Several (heavy) metals are a common component of living organisms, but they can be harmful if accumulate in excess while other metals have no known physiological role. Excess of metals stimulate oxidative stress and metabolic changes in lichens (Pisani et al. 2011; Paoli et al. 2014a; Piovár et al. 2017; Kováčik et al. 2020) and some metabolites may be elevated by the presence of metals (Dresler et al. 2021). Deeper studies focused on the metabolic changes in lichens in relation to “natural” field stress are not available although several works also in Slovakia studied the impact of industrial pollution on lichen diversity by monitoring the occurrence of species (reviewed by Paoli et al. 2021).

There is information on the content of elements in organisms around metallurgical activities in some countries (Koz et al. 2012; Koz 2014; Vitali et al. 2019), however, in Slovakia, deeper studies are rare (Dzubaj et al. 2008). The present study therefore aims to monitor, using common lichen *Xanthoria parietina*, accumulation of 55 elements in lichen samples collected around Slovakia: just the locality which we selected as no. 1 is below the heap of former nickel smelter (~45 ha) which is a long-term environmental problem (Michaeli et al. 2021). Other sites were monitored around this heap to study the spatial distribution of elements, and more distant sites in Slovakia were randomly selected regarding whether they are “probably clean” or “contaminated”. Not only elements were studied, but also several general and specific metabolites, resulting in the most comprehensive study to date. In was therefore the main aim to identify eventual specific metallic profile related to metallurgical contamination and to study how metabolites correlate with the loading of metals. In addition, available data on PM10 particles were obtained from an official institute to identify possible effects on the elements in lichens, and the “substrate” (polymetallic waste) from a former nickel smelter dump was analyzed for elemental profile (see data in Supplementary materials).

2. Materials and methods

2.1. Sites, lichen collection and preparation of samples

Samples of the epiphytic lichen *Xanthoria parietina* were collected below the heap of former nickel smelter near the town Sereď/village Dolná Streda (locality no. 1, see Fig. 1) and from several localities at various distance from this heap (localities no. 2 – 9), aimed at monitoring spatial distribution of elements spreading from that heap. Additional samples from other parts of Slovakia were collected close to ferroalloy factory (locality no. 11) or magnesite processing plant (locality no. 12) and from potentially clean localities, albeit with the eventual impact of nearby urban settlements (no. 10, 13 – 15). However, localities no. 10, 14 and 15 are presumably clean (see Supplementary Table S1). Lichen samples were collected as short branches within August – September 2021 from at least three individual trees (2-3 branches per tree, meaning 6-9 branches per locality, then $n = 3$) available at given sites ca. 2 m above the ground (mainly from branches of *Populus* sp., *Salix* sp., *Sambucus* sp. or *Acer* sp.). Branches were kept outdoor under natural conditions with occasional misting with distilled water aimed at maintaining lichens viable until the quantification of parameters requiring fresh material (ascorbic acid and non-protein thiols), which was done within one week. Thereafter, lichens were carefully removed from branches of individual trees (using plastic forceps to remove eventual contamination by bark which may have various impact on metal content in lichens, e.g. Santitoro et al. 2004) to achieve at least 1 g of homogenous thalli for each sample/tree (thickness, color and the presence of apothecia) subsequently dried at 70 °C to constant weight (samples were not washed during the preparation procedure as reported by other authors, e.g. McDonough et al. 2022). These dry samples were manually crushed to obtain homogenous fragments and aliquots of ~100 mg were used for analyses of elements and additional metabolites (phenols, amino acids and purines). Identity of *Xanthoria parietina* was confirmed by lichen expert Professor Martin Bačkor, DSc. and the remaining specimens are deposited in the collection of the corresponding author of this paper. We will collect samples at metallurgical sites at regular intervals in the future to monitor the temporal dynamics.

2.2. Quantification of elements

Dry lichen samples were mineralized in a mixture consisting of 16% HNO_3 and 30% H_2O_2 (5:2) using a microwave oven speedwave XPERT (Berghof, Eningen, Germany). All measurements were carried out by Agilent 7900 ICP-MS equipped with an octopole-based collision/reaction cell to remove polyatomic interferences. To correct for instrument instability and/or signal drift and non-spectral interferences and to improve both precision and trueness of quantification, an internal standard solution (ISTD) containing 200 μg Rh/L was used in parallel with the liquid samples analyzed. The element quantification accuracy was evaluated using the following certified reference materials (CRMs): GBW 10052 (Green Tea) and GBW07603 (Bush Leaves) purchased from National Institute of Metrology and Institute of Geophysical and Geochemical Exploration (Beijing, China), CRM NCS ZC73015 Milk Powder (National Research Centre for Certified Reference Materials, NRCRM, Beijing, China); P-WBF CRM 12–2-04 Essential and Toxic Elements in Wheat Bread Flour (pb-anal, Kosice, Slovakia); CRM12-2–03 P-Alfalfa Essential and toxic elements in Lucerne (pb-anal, Kosice, Slovakia). Intra-day and inter-day precisions were calculated to assess the overall precision of the method and were determined by analyzing individual CRMs three times during the same day and three days over one month, respectively. The operating conditions, together with the validation of sample preparation and analyte quantification were the same as previously reported (Kováčik et al. 2022, Supplementary Table S2a and S2b).

The enrichment factor (EF) of individual elements was calculated by a formula EF = (S_M/S_{Al}) / (UCC_M/UCC_{Al}), where S_M and S_{Al} indicate the content of the given metal (M) and Al in the sample/S (from Table 1) and UCC_M and UCC_{Al} indicate the content of the given metal (M) and Al in the Earth's Upper Continental Crust (UCC, all values in the same unit). Metal contents in the Earth's Upper Continental Crust come from Taylor and McLennan (1995). Given work does not contain values for Pt and Te which we also quantified so we used available data of 0.599 ppb for Pt and 3 ppb for Te in the UCC (Park et al. 2012, USGS 2017).

2.3. Assay of metabolites

Supernatants for the quantification of ascorbic acid and non-protein thiols were prepared by manual extraction in mortar with 0.1 M HCl (to obtain complete sample disruption), followed by centrifugation and spectrophotometry using bathophenanthroline or Ellman's method, respectively (Kováčik et al. 2020). Parallel blanks were also assayed.

Total soluble phenols and flavonols were manually extracted in 80% aqueous methanol and free amino acids in 60% aqueous ethanol, followed by quantification with the Folin-Ciocalteu, $AlCl_3$ or ninhydrin reagent, respectively (Kováčik et al. 2022).

Purine metabolites (allantoin, hypoxanthine, xanthine and uric acid) were extracted manually in 0.05 M $(NH_4)_2HPO_4$ buffer, followed by sonication at 80 kHz (ELMA Elmasonic P, Germany) and centrifugation at 4400 rpm (Eppendorf Centrifuge 5804 R, Germany). The supernatant was filtered through a 0.45 μm syringe filter (Chromafil Xtra PTFE 45/13, Macherey-Nagel, Germany) and then subjected to HPLC separation (1200 Agilent Technologies, USA) equipped with autosampler, degasser, quaternary pump, thermostat and DAD detector. The system and data were controlled by ChemStation software (B.03.01, 2007). Separation of purine metabolites (PM) were carried out on ODS-2 Hypersil column (250 × 4.6 mm, I.D., 5 μm) at 25 °C and with a mobile phase consisting of 0.05 M $(NH_4)_2HPO_4$ buffer solution (pH 7.76) at a flow rate of 1 mL/min and 20 μL injection volume (Vlassa et al. 2021). The DAD detection wavelengths for allantoin, uric acid, xanthine, and hypoxanthine were 218, 292, 276, and 255 nm, respectively. Technical parameters of working standard solutions are presented in Supplementary Table S3.

2.4. Statistical analyses

All data were tested (at 0.05 level) for normality using a Shapiro-Wilk's test and Levene's test to examine homogeneity of variance. When normality or homogeneity could not be assumed, a

Box-Cox power transformation of the data was employed. In order to scout data structures and identify groups of samples by the similarity of their variables, the principal component analysis (PCA), K-means clustering, and hierarchical cluster analysis (HCA) was performed using the MATLAB® R2022b software package (The MathWorks, Inc., USA); these methods are easy for interpretation of large data sets (Liu et al. 2023). To evaluate the optimal number of clusters using K-means clustering, the Calinski-Harabasz clustering evaluation criterion was used. Concerning HCA, an agglomerative hierarchical algorithm was used, which progressively combines pairs, by measuring Euclidean distances between the clusters. The method of average linkage was selected because it provided the highest cophenetic correlation (0.96). Selecting only a subset of predictor variables to create a reduced PCA model and improve classification performance was employed by determining feature weights using a diagonal adaptation of neighborhood component analysis (NCA). Heat maps and Pearson's correlation analyses (at 0.05 level) were performed using software GraphPad 9.4.1.

3. Results and discussion

3.1. Accumulation of major metals in nickel smelter sludge and their content in lichens

The main elements detected in the sludge were Ni, Cr, Fe, Mn, and Fe accounted for approx. 50% (Supplementary Table S4). Although their abundance may vary within the whole heap (~45 ha), the content we found is similar to values reported by Michaeli et al. (2021), e. g. 28 – 77% Fe, 9 – 24 mg Cr/g or 1 – 3 mg Ni/g. Quantity of other elements is not known and we detected higher amount of Mn, Ti, Co or V (Supplementary Table S4). Amount of U, Cs, Pt or Be was higher in sludge than in common urban soil but the same was not observed for elements such as Th, Ce, Bi, As or Sn (cf. Supplementary Table S4 and Kováčik et al. 2022).

As naturally expected, the accumulation of four major elements in sludge was highest in lichen samples under the heap (Fe > Cr > Ni > Mn, locality no. 1), which could arise from air transport of fine particles from the heap (Table 1). The subsequent high content of these elements was found at sites no. 11 and/or 12, which are near a ferroalloy plant or magnesite mine (Table 1), confirming relation between particles in the air and metal content in lichen. In line with this assumption, the amount of PM10 particles at selected official monitoring localities was the highest near our site no. 12 while localities no. 1 (probably the most polluted) and no. 15 (probably the least polluted) did not vary significantly (Supplementary Fig. S1), suggesting that the composition of PM particles rather than their quantity affects metal content in lichens. In agreement, correlation was observed between elemental profile of *Evernia prunastri* and atmospheric bulk deposition (Loppi and Paoli 2015) and we found a partial correlation between PM10 amount and some elements (Supplementary Fig. S2).

Absolute content of Fe, Ni and Cr in *Xanthoria* samples was even 10-, 40- and 6-times higher at the locality no. 1 than at other potentially contaminated localities (no. 11 and no. 12, Table 1 and Supplementary Table S1), suggesting the uniqueness of biotope under nickel smelter heap. Other localities (including presumably clean site no. 10, 14 and 15) revealed amount of Fe, Ni and Cr (but also of Pb and Mn) comparable or lower than previous local study at urban/agricultural sites using *Xanthoria* in Slovakia (Paoli et al. 2014b, see Table 2 for values). A study using *Hypogymnia physodes* in Slovakia revealed similar amount of Ni and Cr (cf. Tables 1 and 2 with Guttová et al. 2011). The accumulation of Co and Pb was also much higher in samples from the locality no. 1 compared to other sites (Table 1). Guttová et al. (2011) reported that Pb accumulation in *Hypogymnia physodes* decreased over time in Slovakia and we found a much lower Pb content in *Xanthoria* for most localities (Table 1). In line with our data, *Xanthoria* collected close to steelworks contained ca. 25- and 10-times more Ni and Cr compared to control sites (Vitali et al. 2019) and *Xanthoria* from industrial area in Turkey contained 2 – 7-times more Mn, Pb, Fe, Ni or Co than from urban area (Demiray et al. 2012). Our data also suggest that *Xanthoria* accumulates more metals (10-times more Cr and 2-times more Mn) as e. g. grass species collected around our locality no. 12 (Štofejová et al. 2021). Also lichen *Evernia prunastri* contained higher amount of Fe, Cr or Mn in relation to distance from the landfill (Sujetovienė et al. 2019).

An important aspect is the spatial distribution of metals. Due to high area of the heap (locality no. 1) and clouds of dust carrying particles from uncovered parts reported in previous years (Michaeli et al. 2021), it could be expected that the contamination of samples around the heap will also be elevated. Surprisingly, sites no. 2 – 9 located at various distances from the heap revealed much lower amounts of Fe, Cr, Ni, Mn, Co or Pb (Table 1), thus it seems that contamination has decreased probably due to higher vegetation cover on the heap. Local residents also mention less intense dust clouds. Another possible explanation is that rain washes away metal-bearing particles from epiphytic lichens growing further away from the heap ("dilution" effect), but it does not mean that elements "disappeared" from the environment and monitoring of soil and water is needed.

3.2. Amount of essential elements

K was typically the most abundant element (Table 1) and similar amount of K, Ca or Mg has been detected in *Xanthoria* from Turkey (Dörter et al. 2020). Ca amount was within the range previously reported in *Xanthoria* from Slovakia in urban/agricultural areas (1.1 – 1.45 mg/g) with higher amount around cement mill (Paoli et al. 2014b) as we observed close to magnesite mine or quarry (sites no. 10 and 12, Table 1). As naturally expected, Mg was the most accumulated in samples close to magnesite factory (locality no. 12) but it was surprising that K or Ca were the most abundant in samples from locality no. 11 (close to ferroalloy factory, Table 1) because excess of metals typically depletes cations (Kováčik et al. 2018b). Also, data from Turkey revealed no clear impact of industrial versus sub/urban localities on the K amount (Demiray et al. 2012). Correlation analyses revealed that P was clearly neutral while Ca the most positively correlated (Supplementary Fig. S3) though Ca showed positive correlation only with Pb in the previous study in Slovakia around cement mill (Paoli et al. 2014b).

Micronutrients Fe and Mn (including "ultramicronutrient" Ni) were discussed in the previous section due to their direct relation with the locality no. 1. Other micronutrients were present in the descending order Zn > Cu $\geq$ B > Mo for most localities (Table 1). Amount of Cu or Zn was within the range observed in *Xanthoria* or lichens from other countries (Table 2). Interestingly, the presence B was not detected in the sludge (Supplementary Table S4), indicating its origin from the atmosphere at least for the locality no. 1. It also confirms that calculation of the enrichment factor (chapter 3.6.) using UCC values is correct.

3.3. Accumulation of beneficial elements

Within so-called beneficial elements Al, Na, Se, V and Ti (Pilon-Smits et al. 2009; Imtiaz et al. 2015; Muhammad et al. 2019), Co was discussed above. Al is the 3rd most abundant element in the earth's crust and it was often 2nd the most abundant after K (Table 1). Its quantity varied relatively slightly among localities, so it was used as a background element to calculate the enrichment factor (chapter 3.6.) and it showed positive correlation with many elements (Supplementary Fig. S3). The amount of Al we detected is similar to *Xanthoria* samples from Turkey (Dörter et al. 2020) or Spain (Parviainen et al. 2020).

Quantity of Na > V > Se was similar to data from Turkey, but we observed ca. 10-times more Se (Dörter et al. 2020). However, other epiphytic lichens contain similarly higher Se amount (McDonough et al. 2022) so no environmental hazard is expected. Ti is also considered a beneficial element and its amount was similar to data from other countries (Demiray et al. 2012; Dörter et al. 2020).

3.4. Additional common, non-essential or toxic elements

Continental earth's crust contains over 90 elements and many of them therefore interact with living organisms, leading to stimulatory or toxic effect depending on the concentration. Ba was the last of 11 elements reaching an amount above 10 µg/g in almost all localities (Table 1), as also observed in other lichens (Dörter et al. 2020, McDonough et al. 2022). Locality without extensive industry (no. 5) contained over 120 µg Ba/g, which is ca. 3 – 6-times more than at metallurgical localities no. 1 or 11 (Table 1). In agreement, semi/urban localities contained ca. 2-times more Ba than control in *Xanthoria* samples from Spain (Parviainen et al. 2020) so further monitoring is needed. We found no data for Be though the quantity below 0.1 µg Be/g is similar to crops such as parsley (Tanveer and Wang 2019). Alkali metals Li and Cs but not Rb were the most accumulated in samples from the locality no. 11, but their quantity was similar to data from *Xanthoria* in other countries (Dörter et al. 2020; Parviainen et al. 2020).

Some elements are toxic even at low doses and have no known physiological functions in cells. Among them, Cd, As, Sn and Sb (plus Cr and Pb mentioned above) are the most monitored. Cd showed the greatest variation among localities (ca. 50 – 3500 ng/g, Table 1) and the impact of local factors is expected. In agreement, *Xanthoria* samples from industrial area in Turkey contained more Cd (1.4 – 5.4 µg/g) than those from sub/urban areas (ca. 0.18 – 0.85 µg/g, Demiray et al. 2012) and more Cd was detected in *Xanthoria* from cement mill/quarry than in adjacent agricultural areas (Paoli et al. 2014b). The exceptionally high Cd amount we observed at the locality no. 10 (close to protected peatland and national park) was not expected and an active quarry nearby could be an explanation, requiring further local research. It was also an exceptional phenomenon that Cd showed negative correlation with many elements (Supplementary Fig. S3). As and Sn were the most accumulated at the locality no. 1 followed by no. 11, indicating their relation to close source of metallic pollution (Table 1). Similar pattern (up to 10-fold difference of Sn between urban and control locality) was previously found

(Parviainen et al. 2020). Sb has recently been suggested as a tracer of non-exhaust traffic emissions (Parviainen et al. 2020) and it could be possible for our sites no. 1 and 2 which are situated very close to frequent highway (Table 1). Indeed, control samples of *Xanthoria* from Tuscany contained 0.48 μg Sb/g DW (Paoli et al. 2013), which is ca. 10 times less than our site no. 1 (but many other places had similar content, Table 1). Surprisingly, despite the time and space distance, *Xanthoria* collected in 2005 in the 2nd largest Slovak city Košice, where steel mills have been operating for a long time, contained a comparable amount of Sb, but also Al, Fe, Mn and Pb, and the content of these elements was higher in the vicinity of the steel mill (Dzubaj et al. 2008), similarly as we identified in the case of our metallurgical locality no. 1.

Radioactive elements Th and U strongly varied among localities but were not the most accumulated in samples collected close to nuclear power plant (no. 9) as one would expect. Their quantity was higher than in *Xanthoria* from Turkey (Dörter et al. 2020) and mainly occur at the localities close to metallic pollution (no. 1 and 11). Also *Xanthoria* from semi/urban areas in Spain contained ca. 2-times more Th and U than control site (Parviainen et al. 2020).

Abundance of valuable rare metals decreased in order Ag > Pd $\geq$ Pt at most localities and Pt showed the greatest variability (up to 10-fold, Table 1). It was also interesting that Ag or Pd was the most abundant close to metallurgical localities no. 1 and 11 but Pt at localities within High Tatra Mountains (no. 13 and 14). Owing to known contamination of the environment with platinum metals mainly from automotive exhaust converters in urban areas (Cicchella et al. 2020), it remains an open question whether highest Pt amount in High Tatra Mountains may indicate eventual high density of visitors/cars.

Surprisingly, accumulation of W and Re (and also of B mentioned above) was not detected in the sludge (Supplementary Table S4) but it was found in lichens occurring under the smelter heap (locality no. 1) and at all other sites (Table 1), which indicates their origin from the atmosphere and not from the sludge. However, amount of W was at least 10-times higher at the locality no. 11 (ferroalloy factory) that at other sites with mining or metallurgic activities (no. 1 or 12, Table 1), suggesting the processing of specific ore(s). Ruthenium was the only element detected in sludge from nickel smelter heap but not in lichens (cf. Supplementary Table S4 and Table 1) and its presence in the sludge may arise from the processing of nickel ores where it occurs as a by-product (USGS 2008).

3.5. Content of rare earth elements

Rare earth elements (REE) are identified by the IUPAC as a group of 17 elements (Ramos et al. 2016) and some of them may have an adverse effect also in *Xanthoria* (Paoli et al. 2014a). We detected 14 of these elements with the descending quantity Ce > La > Nd > Y > Pr > Sm > Gd > Dy > Er > Yb > Eu > Tb > Ho > Lu (Table 1). *Xanthoria* from Turkey revealed similar order of elements but with lower absolute values (Dörter et al. 2020). Almost the same order has been observed in medicinal plants (Kováčik et al. 2022) but individual elements were much more accumulated here (Table 1), indicating their bioaccumulation in lichens. All elements were most accumulated in the lichen from sites close to metal pollution (no. 11 and 1) and least at the site considered clean (no. 15), which confirms their connection with the processing of various ores. Study using lichen *Ramalina* found that mainly organic cropping increases amount of REE, but values were often similar to our data (Filippini et al. 2020).

3.6. Enrichment factor (EF)

The EF compares the ratio of the studied metal to a geogenic trace metal and benchmarks this ratio against a baseline data ratio (Wu et al. 2021). We selected Al to normalize accumulation of elements as previously used for lichens (Agnan et al. 2013; Wu et al. 2021) and absolute data are comparable between species/countries.

Typically, values of EF over 10 are considered as an indication of anthropogenic contamination though values over 5 have also been considered (Liu et al. 2016; Wu et al. 2021; McDonough et al. 2022). We found EF > 10 at all localities for 12 elements (P, Zn, B, As, Sb, Cd, Ag, Bi, Pd, Pt, Te and Re) and at 12 out of 15 localities for Pb (Supplementary Table S5). Second group of five elements (Fe, Ni, Co, Mn and W) revealed EF > 10 only at one locality typically connected with a metallic pollution, e. g. Fe, Ni and Co at locality no. 1. Third group of six elements includes both essential and toxic ones (K, Mg, Cu, Cr, Sn and Mo) with EF > 10 at two or more localities: only Cr revealed clear relation to mining/metallurgic activities and EF value of 30 – 550 was detected at localities no. 1, 11 and 12 (Supplementary Table S5). The biggest group of 30 elements did not reach EF over 10 with typical value of 1 – 3 (marked by green color in Supplementary Table S5), indicating a geogenic origin (Wu et al. 2021).

In line with our data, report from Australia showed elevated EF for Cd, Cu, Pb and Zn (values 14 – 1211) but only 1 – 4 for Ti and Fe (Wu et al. 2021). In agreement with our values, data from lichens in Canada revealed anthropogenic origin (EF > 10) for Zn, B, As and Sb but not for Cd (McDonough et al. 2022). Additionally, epilithic lichen *Xanthoria mandschurica* in China revealed EF > 10 for P, Zn, Sb and Cd (Liu et al. 2016) so it seems that anthropogenic contamination by some elements is a more general phenomenon throughout the world. We note that we observed the highest EF values for Pd (over 1400) followed by Pt, Sb and Cd (Supplementary Table S5) and further monitoring of given elements over time needs attention. We are aware that local soil values would be more suitable to calculate EF but due to epiphytic nature of given lichen species (and some elements undetected in the sludge but in lichens), we prioritized calculations using UCC values, allowing comparison with studies discussed above.

3.7. Accumulation of metabolites

Various metals have typically various impact on key cellular antioxidants. It was observed in lichens that the impact of metals varies, e. g. vitamin C (ascorbic acid, AsA) and thiols decreased in response to Cu but rather increased under Cr or Ni excess after short (24 h) exposure (Kováčik et al. 2018a and 2018b). We found that the amount of AsA and non-protein thiols was the lowest in samples from localities no. 1 and 11 which are directly affected by metals originated either from sludge heap or from ferroalloy factory (Fig. 2 and Table 1). Correlations confirmed typically negative trend (see also graphical abstract for heat map) but only some values were significant (Supplementary Table S6). It seems that higher load of air-born metals had negative impact on antioxidants mainly close to metallic pollution (Fig. 2). In agreement, previous work confirmed that excess Cd decreases glutathione content and increases phytochelatins (main cellular non-protein thiols) in *Xanthoria*, while the sum of individual substances in the control (Kalinowska et al. 2015) was similar to our NPT content (Fig. 2).

On the contrary to antioxidants, free amino acids were mainly positively correlated with individual metals (Supplementary Table S6) and their accumulation varied (Fig. 2). Positive correlation between protein content and some metals has been observed in lichens from polluted areas in India (Chetia et al. 2021) and increasing trend of protein content was observed in *Ramalina* (Filippini et al. 2020).

The amount of soluble phenols varied more than that of flavonols but was not the lowest at localities with known metallic contamination (Fig. 2 and Supplementary Fig. S4). Though the correlation between soluble phenols and flavonols was positive ($r = 0.45$), their correlations with elements differed strongly and were rather slightly negative for phenols but positive for flavonols (Supplementary Table S6, see also graphical abstract for heat map). One explanation may be the fact that many lichen specific metabolites are of phenolic nature but flavonols/flavonoids are rather present in algal cells within thalli so both chemical structure and quantity of metabolites affect correlations. Unfortunately, we found no similar data in lichens which we could discuss in detail, but our results may be useful for subsequent studies.

Allantoin is a nitrogenous organic metabolite and its amount may correlate with so-called "anthropopressure" level in lichens (Dresler et al. 2021) and other specific metabolites provide protection against other forms of stress impacts (Vannini et al. 2018). Unlike previous data where allantoin was low in two non-urban areas in *Xanthoria* from Poland (ca. 0.6 – 1.2 mg/g, Dresler et al. 2021), we observed higher values at localities no. 10 and 15 (forest) and similar or lower values in samples close to source of metallic contamination (localities no. 1 and 11, Table 3). Surprisingly, the highest allantoin amount (4.4 mg/g) was detected in samples close to nuclear power plant (no. 9) and allantoin showed rather negative correlation with elements (Supplementary Table S7). It seems that bigger set of the analyzed metals we obtained here is more objective in terms of eventual correlations. Subsequent quantification of related metabolites (hypoxanthine and xanthine) revealed their considerable accumulation in samples close to eventual source of metallic contamination (no. 1 or 11) and lower accumulation at locality in High Tatra Mountains (no. 14) but the same was not observed for uric acid (Table 3): for this reason, many elements showed positive correlations with hypo/xanthine but not with uric acid (Supplementary Table S7 and see also graphical abstract for heat map). These data suggest that not allantoin but mainly hypo/xanthine may have a protective function in lichens and further physiological studies will be carried out by our team.

3.8. Cluster and PCA analyses

Separation of localities with respect to elements and metabolites showed 4 and 3 clusters, respectively (Fig. 3). Mainly elements Cr, Fe, Ni, Co, Sb, Pb, W, Ca, Sr, Pd and rare earth elements separated localities no. 1 and 11 from the remaining localities (Fig. 3A). It was interesting to find that e. g. localities no. 2, 5 and 9, which are close to locality no. 1, are in the same cluster as locality no. 12 (magnesite mining/processing), indicating a similar multi-element profile. The biggest cluster no. 2 involves 9 localities including presumably clean localities (no. 10, 14 and 15) so the elemental content in those localities may be considered as "natural" or basic for *Xanthoria parietina* in Slovakia. Subsequent assay of the same elemental data with PCA confirmed separation of localities no. 1 and 11 (metallic activities) from other localities (Supplementary Fig. S5) with respect to main elements (see Supplementary Fig. S6 for heat map of the analyte loadings). Cluster dendrogram (HCA) created using the same 55 elements confirmed result of PCA and sites no. 1 and 11 were clearly separated from others (Supplementary Fig. S7). PCA analyses with reduced number of elements (36 and 28) showed the same clear separation of sites no. 1 and 11 from others and had a positive effect on the total percentage of variation explained by the first two PCs (Supplementary Fig. S8).

Cluster analysis of metabolites revealed three clusters (Fig. 3B). Subsequent PCA analysis of the same data (Supplementary Fig. S9 and S10) revealed that metallurgical localities no. 1 and 11 showed a trend toward separation. Correlation of individual metabolites and elements varied greatly as mentioned above (see also graphical abstract for heat map).

4. Conclusions

Elemental profiling confirmed uniqueness of sites exposed to metallic contamination (below heap of former nickel smelter or close to ferroalloy factory) and samples from these sites were clearly separated from others. Additional localities even close to mentioned heap were not different from other sites throughout Slovakia (some of them considered clean), indicating that i) "normal" metallic content in *Xanthoria* may be established and, ii) particles from heap are not spatially transported or accumulated in lichens at sites further away from the heap (localities no. 2 – 9). This was a very surprising finding suggesting that metallic contamination may be washed out by rain from lichens so further monitoring of vascular species will be carried out.

The enrichment factor calculated using UCC values for 12 elements at all 15 localities was elevated, indicating an anthropogenic contamination. This may be mainly due to intensive metallurgical and chemical industry in the previous decades. Metabolic analyses showed that basic antioxidants are sensitive to higher metal content (negative correlations) while hypoxanthine and xanthine may be protective metabolites (positive correlations) and further physiological studies are needed.

Acknowledgments

The work was supported by Slovak grant agency VEGA (project no. 1/0003/21) and analyses of foreign co-authors also by internal sources of their workplaces. The corresponding author is very thankful to Assoc. Prof. Juraj Hladký, PhD. and MSc. Renáta Szabová (University of Trnava) for their kind help with sample collection.

Author contribution

Experimental design and manuscript preparation (JK), assay of elements (LH, JP and MP), assay of metabolites (JK, MaV, MiV and MF), statistics (JK, MaV and LH) and manuscript revision (LH, MiV and MF).

Disclosure statement

The authors declare that there are no conflicts of interest.

Role of the funding sources

Sponsor had no involvement in the present study.

Data Availability Statement

The data presented in this study are available upon reasonable request from the corresponding author.

References

Agnan, Y., Séjalon-Delmas, N., Probst A. 2013. Comparing early twentieth century and present-day atmospheric pollution in SW France: A story of lichens. Environ. Pollut. 172, 139-148.

Bačkor, M., Paulíková, K., Geralská A., Davidson, R. 2003. Monitoring of air pollution in Košice (Eastern Slovakia) using lichens. Polish J. Environ. Stud. 12, 141-150.

Chetia, J., Gogoi, N., Gogoi, R., Yasmin, F. 2021. Impact of heavy metals on physiological health of lichens growing in differently polluted areas of central Assam, North East India. Plant Physiol. Rep. 26, 210-219.

Cicchella, D., Zuzolo, D., Albanese, S., Fedele, L., Di Tota, I., Guagliardi, I., Thiombane, M., De Vivo, B., Lima, A., 2020. Urban soil contamination in Salerno (Italy): concentrations and patterns of major, minor, trace and ultra-trace elements in soils. J. Geochem. Explor. 213, 106519.

Demiray, A.D., Yolcubal, I., Akyol, N.H., Çobanoğlu, G. 2012. Biomonitoring of airborne metals using the lichen *Xanthoria parietina* in Kocaeli Province, Turkey. Ecol. Indic. 18, 632-643.

Dörter, M., Karadeniz, H., Saklangıçaç, U., Yenisoy-Karakaş, S. 2020. The use of passive lichen biomonitoring in combination with positive matrix factor analysis and stable isotopic ratios to assess the metal pollution sources in throughfall deposition of Bolu plain, Turkey. Ecol. Indic. 113, 106212.

Dresler, S., Kováčik, J., Wójciak, H., Sowa, I., Strzemski, M., Wojciak, M. 2021. Allantoin content in lichens depends on anthropopressure level. Ecol. Indic. 24, 107312.

Dzubaj, A., Bačkor, M., Tomko, J., Peli, E., Tuba, Z. 2008. Tolerance of the lichen *Xanthoria parietina* (L.) Th. Fr. to metal stress. Ecotox. Environ. Safe. 70, 319-326.

Filippini, E., Cañas, M., Acosta, W.D., Plá, R.R., Jasan, R.C., Invernizzi, R., Estrabou, C. 2020. Physiological response and multi-elemental content in lichens growing on agricultural fences: A pilot study comparing no-tillage and organic cropping. Bull. Environ. Contam. Toxicol. 105, 211-217.

Guttová, A., Lackovičová, A., Pišút, I., Pišút, P. 2011. Decrease in air pollution load in urban environment of Bratislava (Slovakia) inferred from accumulation of metal elements in lichens. Environ. Monit. Assess. 182, 361-373.

Imtiaz, M., Rizwan, M.S., Xiong, S., Li, H., Ashraf, M., Shahzad, S.M., Shahzad, H., Rizwan M., Tu S. 2015. Vanadium, recent advancements and research prospects: A review. Environ. Int. 80, 79-88.

Kalinowska, R., Bačkor, M., Pawlik-Skowrońska, B. 2015. Parietin in the tolerant lichen *Xanthoria parietina* (L.) Th. Fr. increases protection of *Trebouxia* photobionts from cadmium excess. Ecol. Indic. 58, 132-138.

Kováčik, J., Dresler, S., Babula, P. 2018a. Metabolic responses of terrestrial macrolichens to nickel. Plant Physiol. Biochem. 127, 32-38.

Kováčik, J., Dresler, S., Peterková, V., Babula, P. 2018b. Metal-induced oxidative stress in terrestrial macrolichens. Chemosphere 203, 402-409.

Kováčik, J., Dresler, S., Babula, P., Hladký, J., Sowa, I. 2020. Calcium has protective impact on cadmium-induced toxicity in lichens. Plant Physiol. Biochem. 156, 591-599.

Kováčik, J., Husáková, L., Graziani, G., Patočka, J., Vydra, M., Rouphael, Y. 2022. Nickel uptake in hydroponics and elemental profile in relation to cultivation reveal variability in three *Hypericum* species. Plant Physiol. Biochem. 185, 357-367.

Koz, B. 2014. Energy-dispersive X-ray fluorescence analysis of moss and soil from abandoned mining of Pb-Zn ores. Environ. Monit. Assess. 186, 5315-5326.

Koz, B., Celik, N., Cevik, U. 2010. Biomonitoring of heavy metals by epiphytic lichen species in Black Sea region of Turkey. Ecol. Indic. 10, 762-765.

Koz, B., Cevik, U., Akbulut, S. 2012. Heavy metal analysis around Murgul (Artvin) copper mining area of Turkey using moss and soil. Ecol. Indic. 20, 17-23.

Kularatne, K.I.A., de Freitas, C.R. 2013. Epiphytic lichens as biomonitors of airborne heavy metal pollution. Environ. Exp. Bot. 88, 24-32.

Liu, J., Kang, H., Tao, W., Li, H., He, D., Ma, L., Tang, H., Wu, S., Yang, K., Li, X. 2023. A spatial distribution – Principal component analysis (SD-PCA) model to assess pollution of heavy metals in soil. Sci. Total Environ. 859, 160112.

Liu, H.J., Zhao, L.C., Fang, S.B., Liu, S.W., Hu, J.S., Wang, L., Liu, X.D., Wu, Q.F. 2016. Use of the lichen *Xanthoria mandschurica* in monitoring atmospheric elemental deposition in the Taihang Mountains, Hebei, China. Sci. Rep. 6, 23456.

Loppi, S., Paoli, L. 2015. Comparison of the trace element content in transplants of the lichen *Evernia prunastri* and in bulk atmospheric deposition: a case study from a low polluted environment (C Italy). Biologia 70, 460-466.

Manninen, S., Jääskeläinen, K., Stephens, A., Iwanicka, A., Tang, S., van Dijk, N. 2023. NH_3 concentrations below the current critical level affect the epiphytic macrolichen communities – Evidence from a Northern European City. Sci. Total. Environ. 877, 162877.

McDonough, A.M., Bird, A.W., Luciani, M.A., Todd, A.K. 2022. Establishing trace element concentrations for lichens and bryophytes in the ring of fire region of the Hudson Bay Lowlands, Ontario, Canada. Environ. Monit. Assess. 194, 226.

Michaeli, E., Solár, V., Maxin, M., Vilček, J., Boltižiar, M. 2021. The nature of the technosols on the waste from nickel production. Sustainability-Basel 13, 406.

Muhammad N., Zvobgo G., Zhang G.-p. 2019. A review: The beneficial effects and possible mechanisms of aluminum on plant growth in acidic soil. J. Integr. Agric. 18, 1518-1528.

Nannoni, F., Santolini, R., Protano, G. 2015. Heavy element accumulation in *Evernia prunastri* lichen transplants around a municipal solid waste landfill in central Italy. Waste Manag. 43, 353-362.

Paoli, L., Fačkovcová, Z., Lackovičová, A., Guttová, A. 2021. Air pollution in Slovakia (Central Europe): a story told by lichens (1960–2020). Biologia 76, 3235-3255.

Paoli, L., Fiorini, E., Munzi, S., Sorbo, S., Basile, A., Loppi, S. 2013. Antimony toxicity in the lichen *Xanthoria parietina* (L.) Th. Fr. Chemosphere 93, 2269-2275.

Paoli, L., Fiorini, E., Munzi, S., Sorbo, S., Basile, A., Loppi, S. 2014a. Uptake and acute toxicity of cerium in the lichen *Xanthoria parietina*. Ecotox. Environ. Safe. 104, 379-385.

Paoli, L., Guttová, A., Grassi, A., Lackovičová, A., Senko, D., Loppi S. 2014b. Biological effects of airborne pollutants released during cement production assessed with lichens (SW Slovakia). Ecol. Indic. 40, 127-135.

Park, J.W., Hu, Z., Gao, S., Campbell, I.H., Gong, H. 2012. Platinum group element abundances in the upper continental crust revisited – New constraints from analyses of Chinese loess. Geochim. Cosmochim. Acta 93, 63-76.

Parviainen, A., Papaslioti, E.M., Casares-Porcel, M., Garrido, C.J. 2020. Antimony as a tracer of non-exhaust traffic emissions in air pollution in Granada (S Spain) using lichen bioindicators. Environ. Pollut. 263, 114482.

Pilon-Smits E.A.H., Quinn C.F., Tapken W., Malagoli M., Schiavon M. 2009. Physiological functions of beneficial elements. Curr. Opin. Plant Biol. 12, 267-274.

Piovár, J., Weidinger, M., Bačkor, M., Bačkorová, M., Lichtscheidl, I. 2017. Short-term influence of Cu, Zn, Ni and Cd excess on metabolism, ultrastructure and distribution of elements in lichen *Xanthoria parietina* (L.) Th. Fr. Ecotox. Environ. Safe. 145, 408-419.

Pisani, T., Munzi, S., Paoli, L., Bačkor, M., Loppi, S. 2011. Physiological effects of arsenic in the lichen *Xanthoria parietina* (L.) Th. Fr. Chemosphere 82, 963-969.

Popovici, V., Bucur, L., Calcan, S.I., Cucolea, E.I., Costache, T., Rambu, D., Schröder, V., Gîrd, C.E., Gherghel, D., Vochita, G., Caraiane, A., Badea, V. 2022. Elemental analysis and in vitro evaluation of antibacterial and antifungal activities of *Usnea barbata* (L.) Weber ex F.H. Wigg from Călimani Mountains, Romania. Plants-Basel 11, 32.

Ramos, S.J., Dinali, G.S., Oliveira, C., Martins, G.C., Moreira, C.G., Siqueira, J.O., Guilherme, L.R.G., 2016. Rare earth elements in the soil environment. Curr. Pollut. Rep. 2, 28-50.

Rola, K., Osyczka, P. 2019. Temporal changes in accumulation of trace metals in vegetative and generative parts of *Xanthoria parietina* lichen thalli and their implications for biomonitoring studies. Ecol. Indic. 96, 293-302.

Santitoro, A., Aprile, G.G., Baldantoni, D., Bartoli, G., Alfani, A. 2004. Trace element analyses in an epiphytic lichen and its bark substrate to assess suitability for air biomonitoring. Environ. Monit. Assess. 98: 59-67.

Sujetovienė, G., Smilgaitis, P., Dagiliūtė, R., Žaltauskaitė J. 2019. Metal accumulation and physiological response of the lichens transplanted near a landfill in central Lithuania. Waste Manag. 85, 60-65.

Štofejová, L., Fazekaš, J., Fazekašová, D. 2021. Analysis of heavy metal content in soil and plants in the dumping ground of magnesite mining factory Jelšava-Lubeník (Slovakia). Sustainability-Basel 13, 4508.

Tanveer, M., Wang, L. 2019. Potential targets to reduce beryllium toxicity in plants: A review. Plant. Physiol. Biochem. 139, 691–696.

Taylor, S.R., McLennan, S.M. 1995. The geochemical evolution of the continental crust. Rev. Geophys. 33, 241-265.

USGS 2008. United States Geological Survey: Platinum-Group Metals Statistics and Information. https://www.usgs.gov/centers/national-minerals-information-center/platinum-group-metals-statistics-and-information

USGS 2017. United States Geological Survey: Tellurium Chapter R of Critical Mineral Resources of the United States – Economic and Environmental Geology and Prospects for Future Supply. https://pubs.er.usgs.gov/publication/pp1802R

Vannini, A., Paoli, L., Ceccarelli, S., Sorbo, S., Basile, A., Carginale, V., Nali, C., Lorenzini, G., Pica, M., Loppi, S. 2018. Physiological and ultrastructural effects of acute ozone fumigation in the lichen *Xanthoria parietina*: the role of parietin and hydration state. Environ. Sci. Pollut. Res. 25, 8104-8112.

Vannini, A. Tedesco, R., Loppi, S., Di Cecco, V., Di Martino, L., Nascimbene, J., Dallo, F., Barbante, C. 2021. Lichens as monitors of the atmospheric deposition of potentially toxic elements in high elevation Mediterranean ecosystems. Sci. Total Environ. 798, 149369.

Vitali, M., Antonucci, A., Owczarek, M., Guidotti, M., Astolfi, M.L., Manigrasso, M., Avino, P., Bhattacharya, B., Protano, C. 2019. Air quality assessment in different environmental scenarios by the determination of typical heavy metals and persistent organic pollutants in native lichen *Xanthoria parietina*. Environ. Pollut. 254, 113013.

Vlassa, M., Filip, M., Dragomir, C. 2021. Solid phase extraction and HPLC-DAD separation and determination of four purine derivatives in cow's milk. Czech J. Food Sci. 39, 122-130.

Wu, L., Isley, C.F., Handley, H.K., Taylor, M.P. 2021. Atmospheric sources of anthropogenic and geogenic trace metals in Australian lichen and fungi. Anthropocene 33, 100279.

Zakrzewska, M., Klimek, B. 2018. Trace element concentrations in tree leaves and lichen collected along a metal pollution gradient near Olkusz (Southern Poland). Bull. Environ. Contam. Toxicol. 100, 245-249.

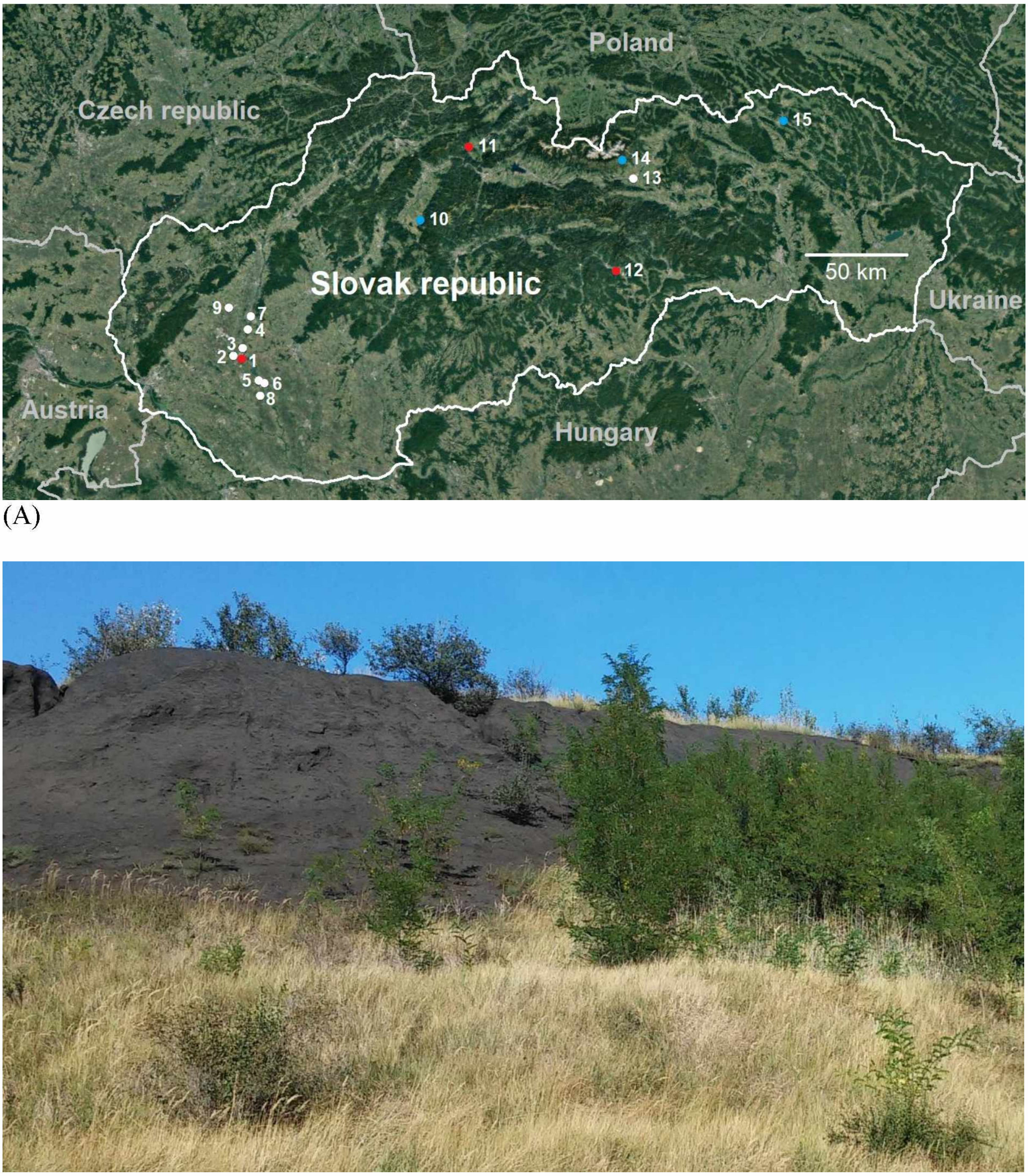

(A)

(B)

Figure 1. A: Map showing the localization of individual sites where samples of epiphytic lichen *Xanthoria parietina* were collected (see Supplementary Table S1 for description of sites). Locality no. 1 is under the heap of former nickel smelter and localities no. 1, 11 and 12 (red color) are considered the most polluted due to metallurgical/mining activities, while sites no. 10, 14 and 15 can be considered clean/control and are in/near forest areas (blue color). The other sites are in urban/rural settlements, but without a clear source of pollution. The map and locations were created using Google maps and the boundaries were highlighted using paint software. B: Photo of the locality no. 1 with visible black sludge from the processing of various ores (sludge contains mainly Ni, Cr, Fe, Mn and Co as shown in the Supplementary Table S4).

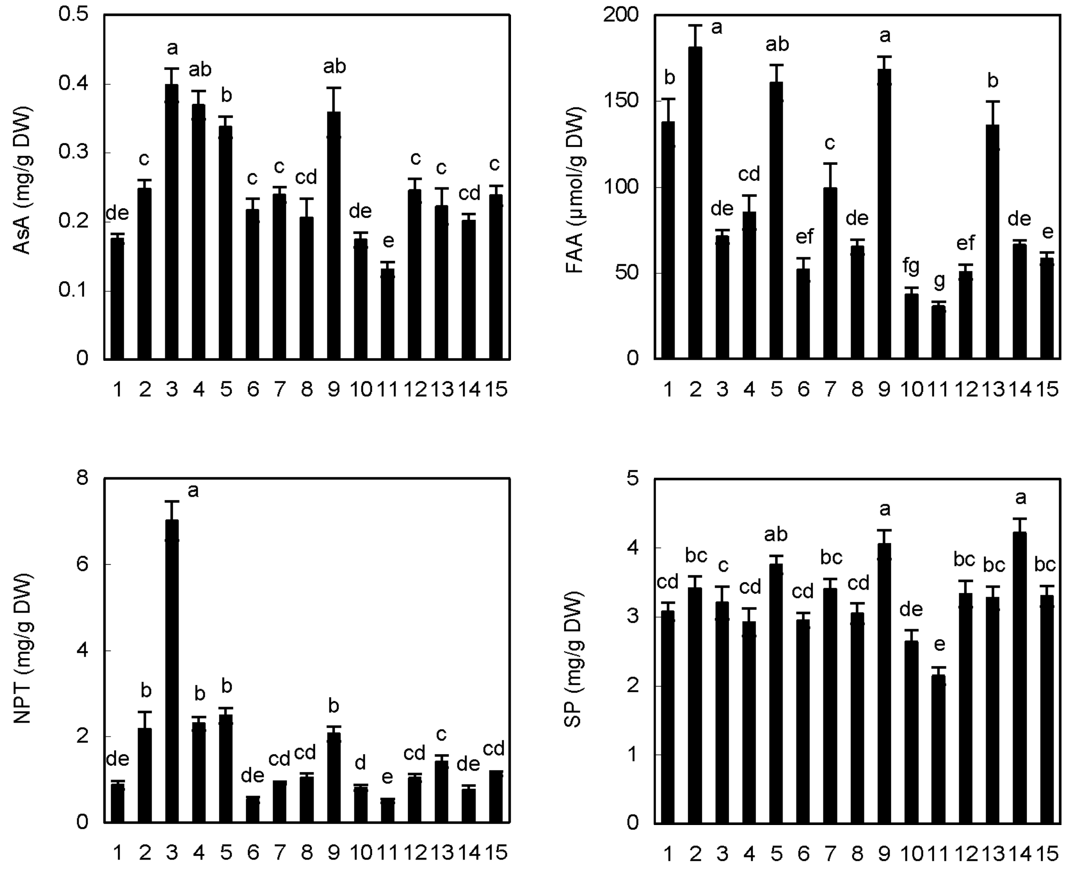

Figure 2. Accumulation of ascorbic acid (AsA, mg/g DW), non-protein thiols (NPT, mg/g DW), free amino acids (FAA, µmol/g DW) and soluble phenols (SP, mg/g DW) in the lichen *Xanthoria parietina* collected at 15 localities within the Slovak Republic. Locality no. 1 is under the heap of former nickel smelter and localities no. 1 and 11 are considered the most polluted due to metallurgical activities, while sites no. 10, 14 and 15 can be considered clean/control (see Fig. 1 for the map with localities and Supplementary Table S1 for description of sites). Data are means ± SDs ($n = 3$). Columns within graph, followed by the same letter(s), are not significantly different according to Tukey's test ($P<0.05$).

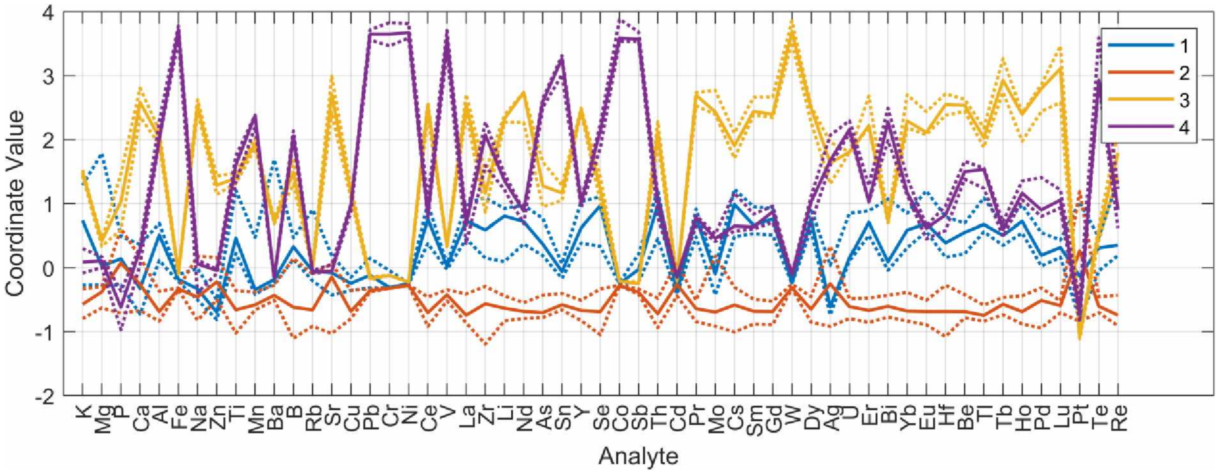

(A)

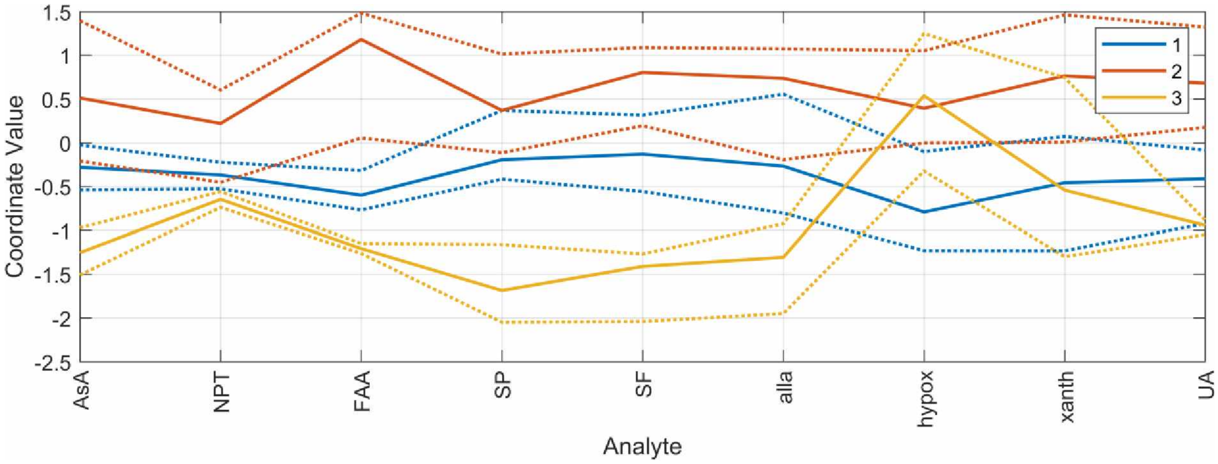

(B)

Figure 3. A: median values of standardized accumulation of individual elements (as solid line and 25-75 percent quartile values as dotted lines) – cluster 4 includes only locality no. 1, cluster 3 includes only locality no. 11 (note that both localities no. 1 and 11 are considered the most polluted due to metallurgic activities but with different quantity of elements, see Table 1), cluster 2 includes localities no. 3, 4, 6, 7, 8, 10, 13, 14 and 15, cluster 1 includes localities no. 2, 5, 9 and 12 (see description of localities in Supplementary Table S1). B: median values of standardized accumulation of individual metabolites – cluster 3 includes localities no. 10 and 11, cluster 2 includes localities no. 1, 2, 3, 5, 7 and 9, cluster 1 includes localities no. 4, 6, 8, 12, 13, 14 and 15. See also Supplementary Fig. S5 and S9 for equivalent PCA graphs of the same data.

Table 1. Accumulation of 55 elements in the lichen *Xanthoria parietina* collected at 15 localities within the Slovak Republic (see Fig. 1 for the map with localities and Supplementary Table S1 for description of sites). Locality no. 1 is under the heap of the former nickel smelter and localities no. 1 and 11 are considered the most polluted due to metallurgical activities, while sites no. 10, 14 and 15 can be considered clean/control. Elements are listed based on their quantity in lichen samples from the locality no. 15 (typically the lowest accumulation among all monitored localities) and the order of localities is based on the distance from the locality no. 1. Data are means (*n* = 3) and for the lucidity of table, SDs are not shown (all values are per gram of dry weight). Values within rows, followed by the same letter(s), are not significantly different according to Tukey's test (P<0.05). ^{X} sum of rare earth elements (REE) and sum of all detected elements are shown as µg/g and mg/g, respectively. The highest value is marked in bold and the dominance of metallurgical sites (no. 1 and 11) is visible.

	1	2	3	4	5	6	7	8	9	10	11	12	13	14	15
K (mg/g)	4.65^{b}	5.76^{a}	3.99^{bc}	2.97^{d}	5.84^{a}	3.76^{c}	4.10^{bc}	3.85^{c}	4.71^{b}	3.97^{c}	**5.98^{a}**	4.09^{bc}	4.33^{bc}	3.88^{c}	**6.27^{a}**
Mg (mg/g)	1.80^{bc}	1.55^{cd}	1.43^{d}	0.96^{e}	1.92^{bc}	1.15^{e}	1.12^{e}	1.46^{cd}	1.30^{de}	1.72^{c}	2.12^{b}	**5.44^{a}**	1.39^{d}	0.93^{e}	1.30^{de}
P (mg/g)	1.01^{bc}	1.23^{abc}	1.06^{bc}	0.58^{d}	1.34^{ab}	0.92^{c}	1.26^{ab}	1.10^{bc}	1.04^{bc}	1.16^{b}	1.43^{ab}	1.17^{b}	**1.50^{a}**	**1.54^{a}**	1.23^{ab}
Ca (mg/g)	1.61^{cd}	1.29^{de}	1.56^{cd}	1.16^{e}	1.27^{de}	1.43^{d}	1.76^{bc}	0.83^{ef}	0.82^{ef}	2.07^{bc}	**3.11^{a}**	2.26^{b}	1.32^{de}	1.12^{de}	0.63^{f}
Al (mg/g)	**2.93^{a}**	1.87^{b}	0.89^{d}	1.28^{c}	1.85^{b}	1.04^{cd}	0.83^{d}	0.98^{cd}	1.87^{b}	0.97^{d}	**2.87^{a}**	1.30^{c}	1.22^{cd}	1.20^{cd}	0.53^{e}
Fe (mg/g)	**24.5^{a}**	1.45^{d}	0.72^{e}	0.85^{e}	1.80^{c}	0.72^{e}	0.69^{ef}	0.58^{f}	1.36^{d}	0.67^{ef}	2.17^{bc}	2.38^{b}	1.22^{d}	0.81^{e}	0.47^{f}
Na (µg/g)	146.2^{cd}	191.0^{c}	97.1^{ef}	151.4^{cd}	121.1^{de}	143.6^{cd}	113.8^{d}	89.3^{f}	115.4^{d}	116.9^{d}	**335.5^{a}**	136.4^{cd}	215.1^{c}	271.2^{b}	71.0^{f}
Zn (µg/g)	36.2^{c}	23.6^{d}	29.4^{cd}	30.9^{cd}	20.8^{de}	38.7^{c}	35.9^{c}	12.0^{f}	17.9^{ef}	**84.4^{a}**	66.1^{b}	29.9^{cd}	25.1^{d}	**84.8^{a}**	26.5^{cd}
Ti (µg/g)	**96.0^{a}**	**102.7^{a}**	36.9^{e}	49.4^{d}	65.2^{c}	46.9^{d}	34.8^{e}	39.5^{e}	78.2^{b}	45.0^{de}	**92.4^{a}**	60.8^{cd}	58.7^{cd}	62.3^{c}	25.2^{f}
Mn (µg/g)	**144.5^{a}**	26.6^{c}	17.8^{e}	16.3^{ef}	32.0^{c}	18.1^{de}	25.8^{cd}	15.5^{ef}	25.6^{c}	29.8^{c}	128.7^{ab}	112.1^{b}	30.5^{c}	29.5^{c}	12.2^{f}
Ba (µg/g)	19.8^{cd}	19.7^{cd}	13.6^{e}	12.7^{e}	**120.9^{a}**	11.5^{e}	10.8^{e}	16.7^{d}	19.2^{d}	10.4^{e}	44.0^{b}	16.6^{d}	18.3^{d}	25.7^{c}	7.52^{f}
B (µg/g)	**5.93^{a}**	4.51^{bc}	3.39^{cd}	2.86^{d}	4.24^{c}	2.97^{d}	3.96^{c}	2.61^{d}	4.18^{c}	3.90^{cd}	5.37^{ab}	3.76^{cd}	4.14^{c}	2.90^{d}	4.45^{bc}
Rb (µg/g)	6.60^{c}	6.56^{c}	3.39^{f}	4.79^{e}	6.76^{c}	14.0^{a}	3.89^{ef}	3.86^{ef}	5.63^{cd}	11.4^{b}	6.85^{c}	**15.9^{a}**	4.97^{de}	6.28^{c}	3.49^{f}
Sr (µg/g)	6.73^{cd}	6.17^{de}	6.71^{cd}	5.67^{ef}	7.30^{c}	6.71^{cd}	7.08^{c}	3.60^{g}	4.83^{f}	3.53^{g}	**14.5^{a}**	7.18^{c}	6.61^{cd}	11.3^{b}	3.37^{g}
Cu (µg/g)	8.29^{b}	5.13^{c}	3.15^{fg}	4.06^{de}	4.79^{cd}	3.09^{fg}	3.85^{de}	2.70^{g}	4.45^{cd}	3.62^{ef}	9.04^{b}	4.23^{d}	8.78^{b}	**13.7^{a}**	2.64^{g}
Pb (µg/g)	**139.7^{a}**	23.1^{b}	6.17^{d}	3.71^{fg}	19.0^{b}	3.37^{gh}	4.79^{ef}	3.04^{gh}	3.77^{fg}	2.76^{hi}	9.65^{c}	5.40^{de}	2.85^{hi}	1.78^{j}	1.86^{j}
Cr (µg/g)	**702.8^{a}**	4.52^{d}	2.46^{fg}	2.49^{fg}	3.87^{de}	2.12^{gh}	1.90^{gh}	2.10^{gh}	3.09^{ef}	1.66^{hi}	37.4^{c}	112.3^{b}	3.07^{ef}	1.59^{hi}	1.30^{i}
Ni (µg/g)	**149.7^{a}**	2.30^{cd}	1.71^{de}	1.86^{de}	2.66^{bc}	1.31^{ef}	1.61^{ef}	1.18^{f}	2.10^{cd}	1.29^{ef}	3.27^{b}	2.36^{cd}	1.44^{ef}	1.12^{f}	1.20^{ef}
Ce (µg/g)	3.76^{b}	3.82^{b}	1.60^{d}	2.32^{cd}	3.47^{b}	1.83^{d}	1.57^{d}	1.44^{de}	3.87^{b}	1.76^{d}	**5.78^{a}**	2.81^{c}	2.54^{c}	1.86^{d}	1.03^{e}
V (µg/g)	**14.3^{a}**	3.20^{c}	1.47^{de}	1.98^{d}	3.00^{c}	1.52^{d}	1.54^{d}	1.46^{de}	3.10^{c}	1.45^{de}	4.08^{b}	2.97^{c}	2.04^{d}	2.15^{d}	0.84^{e}
La (µg/g)	1.63^{bc}	1.82^{b}	0.73^{de}	1.07^{d}	1.67^{bc}	0.89^{d}	1.02^{d}	0.68^{ef}	1.95^{b}	0.78^{de}	**2.87^{a}**	1.47^{c}	1.09^{d}	0.81^{de}	0.50^{f}
Zr (µg/g)	**1.62^{a}**	1.07^{bc}	0.51^{e}	0.74^{cd}	0.89^{cd}	0.72^{cd}	0.62^{de}	0.50^{e}	1.27^{b}	0.80^{cd}	1.35^{ab}	1.36^{ab}	0.98^{c}	1.06^{bc}	0.46^{e}
Li (µg/g)	1.44^{ab}	1.25^{b}	0.57^{d}	0.88^{c}	1.26^{b}	0.65^{cd}	0.59^{d}	0.65^{cd}	1.23^{b}	0.54^{d}	**1.85^{a}**	0.72^{cd}	0.74^{cd}	0.69^{cd}	0.34^{e}
Nd (µg/g)	0.93^{bc}	0.98^{bc}	0.42^{de}	0.53^{d}	0.86^{bc}	0.46^{de}	0.47^{de}	0.40^{ef}	1.03^{b}	0.44^{de}	**1.49^{a}**	0.75^{c}	0.62^{cd}	0.49^{d}	0.28^{f}
As (µg/g)	**1.88^{a}**	0.86^{c}	0.56^{de}	0.61^{de}	0.95^{c}	0.46^{ef}	0.42^{ef}	0.37^{fg}	0.78^{cd}	0.59^{de}	1.31^{ab}	1.28^{b}	0.47^{de}	0.41^{ef}	0.25^{g}

Sn (µg/g)	**2.28^{a}**	0.70^{d}	0.28^{fg}	0.39^{ef}	0.62^{d}	0.30^{f}	0.32^{f}
Y (µg/g)	0.74^{bc}	0.68^{bc}	0.29^{e}	0.40^{d}	0.57^{c}	0.35^{de}	0.33^{de}
Se (µg/g)	**0.59^{a}**	0.47^{b}	0.28^{cd}	0.30^{cd}	0.43^{b}	0.24^{d}	0.29^{cd}
Co (µg/g)	**29.7^{a}**	0.47^{cd}	0.27^{e}	0.28^{e}	0.50^{c}	0.24^{ef}	0.30^{e}
Sb (µg/g)	**4.94^{a}**	1.15^{b}	0.31^{ef}	0.23^{gh}	0.73^{c}	0.25^{fg}	0.17^{h}
Th (ng/g)	459.2^{bc}	487.6^{bc}	203.1^{f}	276.1^{de}	430.8^{c}	226.6^{ef}	213.0^{f}
Cd (ng/g)	295.7^{c}	92.3^{d}	471.2^{b}	210.6^{c}	110.7^{d}	512.4^{b}	447.8^{b}
Pr (ng/g)	340.6^{b}	360.2^{b}	163.1^{de}	223.1^{cd}	335.4^{b}	169.1^{de}	176.3^{de}
Mo (ng/g)	371.8^{c}	272.3^{d}	140.5^{f}	132.0^{fg}	298.6^{d}	110.1^{g}	152.3^{f}
Cs (ng/g)	248.4^{b}	263.9^{b}	119.4^{e}	175.5^{cd}	265.2^{b}	165.8^{cd}	126.3^{de}
Sm (ng/g)	259.2^{b}	270.8^{b}	123.1^{cd}	158.4^{cd}	252.3^{b}	127.6^{cd}	140.5^{cd}
Gd (ng/g)	197.3^{bc}	190.6^{bc}	86.5^{de}	113.7^{d}	176.9^{c}	90.8^{de}	95.6^{de}
W (ng/g)	138.4^{b}	103.0^{c}	53.3^{e}	55.7^{e}	81.0^{d}	58.8^{e}	76.5^{d}
Dy (ng/g)	173.4^{b}	172.5^{b}	73.0^{d}	107.6^{c}	150.1^{b}	86.5^{cd}	87.2^{cd}
Ag (ng/g)	**39.1^{a}**	18.6^{de}	17.3^{de}	18.2^{de}	19.5^{cd}	24.7^{c}	26.1^{bc}
U (ng/g)	**178.6^{a}**	82.2^{c}	40.3^{e}	52.0^{d}	82.1^{c}	44.8^{de}	53.0^{d}
Er (ng/g)	96.0^{b}	83.2^{cd}	37.5^{f}	53.8^{e}	72.3^{d}	42.8^{f}	42.6^{f}
Bi (ng/g)	**154.5^{a}**	58.3^{cd}	29.7^{g}	36.1^{fg}	64.4^{c}	31.6^{g}	45.2^{ef}
Yb (ng/g)	84.5^{b}	67.6^{c}	30.7^{f}	45.4^{e}	56.2^{d}	38.1^{ef}	32.2^{f}
Eu (ng/g)	60.2^{c}	59.3^{c}	30.5^{e}	34.1^{de}	84.9^{b}	29.1^{e}	29.4^{e}
Hf (ng/g)	55.7^{bc}	63.0^{b}	17.3^{fg}	29.5^{d}	44.2^{c}	25.7^{de}	29.5^{d}
Be (ng/g)	71.9^{b}	54.1^{c}	26.2^{e}	34.7^{de}	52.4^{c}	30.2^{e}	26.1^{e}
Tl (ng/g)	54.6^{b}	51.2^{b}	19.5^{de}	25.4^{d}	40.3^{c}	20.6^{de}	20.5^{de}
Tb (ng/g)	32.7^{b}	32.3^{b}	14.8^{c}	17.6^{c}	29.5^{b}	15.8^{c}	17.0^{c}
Ho (ng/g)	34.6^{b}	31.5^{bc}	14.2^{d}	18.2^{d}	26.5^{c}	16.3^{d}	16.8^{d}
Pd (ng/g)	25.8^{b}	17.9^{c}	14.1^{cd}	13.2^{de}	18.6^{c}	14.6^{cd}	16.3^{cd}
Lu (ng/g)	14.0^{b}	9.64^{c}	4.69^{fg}	6.27^{d}	9.43^{c}	5.32^{ef}	4.65^{fg}
Pt (ng/g)	5.62^{de}	18.2^{bc}	6.85^{d}	14.1^{c}	21.3^{ab}	4.69^{e}	1.72^{g}
Te (ng/g)	**12.4^{a}**	3.09^{d}	1.90^{e}	3.21^{d}	4.58^{bc}	3.54^{d}	2.12^{e}
Re (ng/g)	0.21^{bc}	0.15^{cd}	0.09^{ef}	0.08^{ef}	0.16^{cd}	0.13^{de}	0.10^{e}
sum REE ^{x}	8.37^{b}	8.60^{b}	3.64^{g}	5.13^{de}	7.73^{bc}	4.17^{fg}	4.03^{fg}
sum all ^{x}	**38.0^{a}**	13.6^{c}	9.90^{de}	8.12^{e}	14.4^{c}	9.35^{de}	10.0^{de}

0.21^{g}	0.52^{de}	0.33^{f}	1.22^{b}	0.53^{de}	0.87^{c}	0.44^{e}	0.17^{g}
0.32^{de}	0.61^{c}	0.30^{e}	**1.10^{a}**	0.80^{b}	0.37^{de}	0.39^{d}	0.16^{f}
0.19^{de}	0.46^{b}	0.22^{d}	0.48^{b}	0.32^{c}	0.26^{cd}	0.19^{de}	0.15^{e}
0.21^{f}	0.38^{de}	0.32^{de}	0.76^{b}	0.77^{b}	0.31^{e}	0.41^{d}	0.13^{g}
0.14^{hi}	0.26^{fg}	0.18^{h}	0.37^{e}	0.54^{d}	0.29^{ef}	0.18^{h}	0.11^{i}
195.8^{fg}	502.5^{b}	227.0^{ef}	**629.3^{a}**	347.9^{d}	281.7^{de}	163.5^{g}	136.0^{g}
40.5^{f}	55.2^{e}	**3499.0^{a}**	256.9^{c}	104.3^{d}	48.6^{ef}	44.2^{f}	127.9^{d}
152.3^{e}	359.8^{b}	175.2^{de}	**566.7^{a}**	279.8^{c}	212.6^{d}	174.1^{de}	108.3^{f}
302.0^{d}	166.8^{ef}	218.1^{e}	**753.7^{a}**	262.6^{de}	539.5^{b}	487.3^{b}	93.9^{g}
134.2^{de}	269.4^{ab}	147.7^{cd}	**320.6^{a}**	196.4^{c}	173.8^{cd}	176.2^{cd}	79.6^{f}
115.9^{d}	289.2^{b}	124.8^{cd}	**424.0^{a}**	237.7^{b}	175.2^{c}	141.9^{cd}	76.2^{e}
81.3^{e}	219.2^{b}	88.7^{de}	**309.4^{a}**	182.1^{bc}	115.6^{d}	103.3^{d}	59.2^{f}
52.8^{e}	81.7^{d}	89.6^{cd}	**1655.9^{a}**	100.2^{c}	88.9^{cd}	53.7^{e}	54.8^{e}
81.0^{cd}	169.7^{b}	73.3^{d}	**255.9^{a}**	165.4^{b}	99.3^{c}	100.4^{c}	44.8^{e}
14.8^{e}	21.1^{cd}	23.9^{c}	37.7^{ab}	31.5^{b}	18.8^{de}	32.3^{ab}	31.4^{b}
44.5^{de}	85.3^{c}	52.7^{d}	160.6^{ab}	145.4^{b}	58.4^{d}	45.9^{de}	28.0^{f}
41.3^{f}	83.7^{cd}	38.4^{f}	**133.2^{a}**	92.1^{bc}	48.9^{ef}	51.3^{e}	23.4^{g}
21.2^{h}	53.9^{de}	33.7^{g}	90.3^{b}	157.1^{a}	46.7^{e}	29.0^{gh}	21.5^{h}
36.1^{f}	68.3^{c}	35.2^{f}	**113.5^{a}**	78.5^{bc}	49.1^{de}	47.8^{de}	18.3^{g}
28.5^{e}	61.4^{c}	27.3^{e}	**99.7^{a}**	66.2^{c}	37.1^{d}	40.9^{d}	15.8^{f}
21.3^{ef}	46.7^{c}	34.4^{cd}	**90.5^{a}**	47.1^{c}	47.8^{c}	40.6^{cd}	14.6^{g}
27.6^{e}	53.5^{c}	28.2^{e}	**92.8^{a}**	41.2^{d}	32.8^{de}	25.0^{e}	13.8^{f}
19.9^{de}	40.2^{c}	21.5^{de}	**64.7^{a}**	46.6^{bc}	18.1^{de}	16.4^{ef}	12.3^{f}
15.2^{c}	33.4^{b}	15.9^{c}	**65.4^{a}**	30.5^{b}	19.3^{c}	19.0^{c}	8.41^{d}
16.4^{d}	30.1^{bc}	15.0^{d}	**44.6^{a}**	32.2^{bc}	18.1^{d}	17.6^{d}	8.15^{e}
10.2^{ef}	18.1^{c}	9.22^{ef}	**38.2^{a}**	25.5^{b}	12.8^{d}	19.8^{c}	7.35^{f}
5.03^{ef}	9.92^{c}	4.97^{ef}	**24.3^{a}**	11.4^{bc}	5.49^{de}	6.11^{d}	3.64^{g}
16.8^{bc}	4.56^{e}	**24.8^{a}**	2.17^{g}	4.48^{e}	**24.9^{a}**	22.0^{ab}	3.19^{f}
1.66^{e}	3.95^{cd}	1.58^{e}	4.97^{b}	5.17^{b}	1.66^{e}	0.70^{f}	1.72^{e}
0.09^{ef}	**0.29^{a}**	0.15^{cd}	0.27^{ab}	0.20^{bc}	0.08^{ef}	0.08^{ef}	0.06^{f}
3.42^{g}	8.81^{b}	3.96^{fg}	**13.2^{a}**	7.08^{c}	5.42^{d}	4.25^{ef}	2.35^{h}
9.02^{de}	11.4^{d}	10.9^{d}	18.4^{b}	17.2^{b}	11.3^{d}	10.0^{de}	10.6^{de}

Table 2. Accumulation of selected elements in selected epiphytic lichens (µg/g). The data presented graphically in the works cited were read as accurately as possible. The range often includes control and polluted sites, so the highest quantities are usually located near the potential source of pollution (e. g. landfill, refineries, steel mills or quarry). * indicates epilithic species, nd – not detected.

species	country	element	amount	reference
Xanthoria parietina	Poland	Ni, Cr, Cd, Pb	0.2 – 1, 0.5 – 3.2, 0.065 – 0.6, 1 – 10	Rola and Osyczka 2019
		Cu, Zn	4 – 25, 28 – 70	
Xanthoria parietina	Spain	Ni, Cr, Mn, Co, Cd	3.5 – 12, 5.7 – 13, 74 – 75, 0.83 – 1.4, 0.09 – 0.15	Parviainen et al. 2020
		Th, U, Sn	0.41 – 0.85, 0.22 – 0.41, 0.25 – 2.3	
Xanthoria parietina	Italy	Ni, Cr, Co, Cd	1.03 – 43.58, 2.87 – 51.87, 1.03 – 4.65, 0.08 – 0.72	Vitali et al. 2019
		Pb, As	1.08 – 6.89, 0.05 – 0.83	
Xanthoria parietina	Turkey	Ni, Mn, Co, Cd, Pb	2.7 – 20.0, 40 – 1022, 0.54 – 3.21, 0.18 – 5.39, 8 – 394	Demiray et al. 2012
		Cu, Zn, Ti, Tl, V	8 – 694, 65 – 1678, 13 – 118, 0.02 – 0.37, 3 – 23	
Xanthoria parietina	Turkey	Ni, Cr, Mn, Co, Pb	1.97, 3.35 – 3.85, 27.7 – 29.3, 0.56, 1.12 – 1.21	Dörter et al. 2020
		Th, U, Ba, Mo, W	0.15 – 0.17, 0.059 – 0.065, 0.095 – 0.12, 0.038 – 0.041	
Xanthoria parietina	France	Mn, Co, Cd, Pb	15 – 48, 0.28 – 0.41, 0.04 – 0.14, 1.9 – 8.4	Agnan et al. 2013
		Cu, Zn, Ti, As, V	4.7 – 7.8, 19 – 31, 53 – 110, 0.5 – 1.3, 2.3 – 3.0	
Xanthoria parietina	Slovakia	Ni, Cr, Mn, Pb, Cd	2.1 – 4.1, 1.6 – 2.8, 17 – 89, 1.6 – 3.4, 0.21 – 0.30	Paoli et al. 2014b
		Cu, Zn, Ti, As, V	3.3 – 4.6, 30 – 46, 18 – 296, 0.37 – 0.83, 0.7 – 6.4	
_Xanthoria mandschurica_*	China	Ni, Cr, Mn, Co, Cd	13.4, 202.2, 261.6, 2.8, 1.05	Liu et al. 2016
		Ce, La, Sm, Th, Cs	17.8, 8.9, 1.5, 3.0, 1.3	
Evernia prunastri	Italy	Ni, Cr, Co, Cd, Pb	2.1 – 3.5, 1.6 – 8.7, 0.22 – 0.4, 0.05 – 0.12, 2.3 – 9.7	Nannoni et al. 2015
		Cu, Zn, As, V	3.7 – 9.4, 17.2 – 52.9, 0.2 – 0.25, 1.3 – 1.7	
Evernia prunastri	Lithuania	Cr, Mn, Cd	5.84 – 10.52, 8.92 – 16.33, 0.02 – 2.84	Sujetovienė et al. 2019
		Fe	31.19 – 110.37	
Evernia mesomorpha	Canada	Ni, Cr, Mn, Co, Cd	0.76, 0.57, 54.7, 0.08, 0.31	McDonough et al. 2022
		Cu, Zn, Ti, Tl, V	1.7, 24.6, 17.5, 0,01, 0.7	
Usnea barbata	Romania	Ni, Cr, Mn, Co, Cd	0.45, 1.0, 101.4, nd, nd	Popovici et al. 2022
		Pb, Zn, Tl, V, Pt	1.3, 20.5, nd, 0.24, nd	
Hypogymnia physodes	Slovakia	Ni, Cr, Mn, Pb	0.14 – 3.04, 0.4 – 8.6, 21 – 524, 6.9 – 34.7	Guttová et al. 2011
		Cu, Zn	1.6 – 12.4, 40 – 662	

Table 3. Accumulation of purine metabolites (µg/g DW) in the lichen *Xanthoria parietina* collected at 15 localities within the Slovak Republic (see Fig. 1 for the map with localities and Supplementary Table S1 for description of sites). Data are means ± SDs (*n* = 3). Values within columns, followed by the same letter(s), are not significantly different according to Tukey's test (P<0.05). Locality no. 1 is under the heap of the former nickel smelter and localities no. 1 and 11 are considered the most polluted due to metallurgical activities, while sites no. 10, 14 and 15 can be considered clean/control.

locality no.	allantoin	hypoxanthine	xanthine	uric acid
1	2515.4 ± 394.1^{e}	98.9 ± 9.98^{a}	63.2 ± 5.56^{abc}	23.9 ± 3.61^{b}
2	3945.0 ± 521.6^{ab}	80.6 ± 4.82^{cd}	71.6 ± 4.45^{a}	18.4 ± 2.70^{bc}
3	2847.3 ± 124.1^{de}	93.3 ± 6.40^{ab}	51.0 ± 2.55^{ef}	17.0 ± 3.03^{cd}
4	3920.5 ± 352.2^{ab}	60.9 ± 1.64^{fg}	54.8 ± 3.47^{de}	16.1 ± 1.12^{cd}
5	3993.5 ± 284.2^{ab}	68.7 ± 2.71^{ef}	44.9 ± 5.15^{fg}	15.2 ± 3.36^{cd}
6	2381.6 ± 76.9^{e}	69.0 ± 4.42^{ef}	29.8 ± 3.59^{h}	8.15 ± 0.95^{f}
7	3697.5 ± 385.6^{b}	80.9 ± 3.17^{cd}	58.8 ± 3.37^{cd}	36.7 ± 4.30^{a}
8	3564.3 ± 153.3^{bc}	64.8 ± 4.25^{fg}	41.3 ± 2.89^{g}	12.5 ± 2.33^{de}
9	4423.2 ± 340.4^{a}	81.1 ± 2.35^{cd}	68.6 ± 4.41^{ab}	25.3 ± 1.82^{b}
10	2348.0 ± 83.6^{e}	75.2 ± 5.83^{de}	32.4 ± 1.96^{h}	8.49 ± 0.84^{ef}
11	1472.0 ± 246.7^{f}	94.3 ± 7.58^{ab}	58.5 ± 6.22^{cd}	7.53 ± 0.83^{f}
12	3082.9 ± 338.7^{cd}	86.2 ± 5.12^{bc}	48.2 ± 4.10^{efg}	14.2 ± 2.56^{cd}
13	3922.0 ± 407.6^{ab}	75.4 ± 5.70^{de}	45.7 ± 4.72^{fg}	15.1 ± 1.82^{cd}
14	2467.1 ± 308.0^{e}	58.1 ± 3.94^{g}	31.0 ± 2.48^{h}	7.50 ± 0.76^{f}
15	2450.9 ± 149.5^{e}	76.4 ± 6.63^{cde}	50.2 ± 5.74^{ef}	8.74 ± 1.27^{ef}

Supplementary Material

Declaration of interests

☐ The authors declare that they have no known competing financial interests or personal relationships that could have appeared to influence the work reported in this paper.

☐~~The authors declare the following financial interests/personal relationships which may be considered as potential competing interests:~~

Author Contributions Statement

Author contribution

Experimental design and manuscript preparation (JK), assay of elements (LH, JP and MP), assay of metabolites (JK, MaV, MiV and MF), statistics (JK, MaV and LH) and manuscript revision (LH, MiV and MF).